

Parametric second Stokes Raman laser output pulse shortening to 300 ps due to depletion of pumping of intracavity Raman conversion

S. N. Smetanin^{1,2} · M. Jelínek³  · V. Kubeček³ · H. Jelínková³ · L. I. Ivleva¹

Received: 12 April 2016 / Accepted: 19 September 2016 / Published online: 30 September 2016
© Springer-Verlag Berlin Heidelberg 2016

Abstract A new effect of the pulse shortening of the parametrically generated radiation down to hundreds of picosecond via depletion of pumping of intracavity Raman conversion in the miniature passively Q-switched Nd:SrMoO₄ parametric self-Raman laser with the increasing energy of the shortened pulse under pulsed pumping by a high-power laser diode bar is demonstrated. The theoretical estimation of the depletion stage duration of the convertible fundamental laser radiation via intracavity Raman conversion is in agreement with the experimentally demonstrated duration of the parametrically generated pulse. Using the mathematical modeling of the pulse shortening quality and quantity deterioration is disclosed, and the solution ways are found by the optimization of the laser parameters.

1 Introduction

A new wave of interest in the compact crystalline Raman lasers rekindled in last years. It is caused firstly by the progress in stimulated Raman scattering (SRS) in crystals under pico- and femtosecond laser pumping and secondly by the appearance of new perspective crystalline Raman-active media [1–7]. A special attention is paid

to all-solid-state lasers in which one active crystal serves both as lasing and SRS-active medium. There are several crystals with such unique properties—tungstates, molybdates, and vanadates activated by rare earth ions for effective lasers with SRS self-conversion (self-Raman lasers) [4–7]. The SRS conversion is usually achieved using a high-Q laser cavity not only for the fundamental laser radiation but also for the SRS radiation components. Using the Q-switched regime together with the output coupler having lower reflectivity for the SRS radiation allows to increase the output SRS radiation pulse energy and simultaneously decrease its duration down to 0.5–1 ns [4–6] owing to the nonlinear (SRS) cavity dumping effect [8].

In [9], we have proposed and demonstrated a new method of the output pulse shortening in the crystalline parametric self-Raman laser in which the nonlinear cavity dumping occurs for the parametrically generated frequency components of the laser radiation. Distinctive feature of the proposed method is that under strong depletion of the fundamental laser radiation owing to the SRS conversion to the first Stokes Raman component the parametrical generation of the next, second Stokes Raman component takes place only in the temporal region where the fundamental laser radiation pulse overlaps with the first Stokes SRS component pulse. Therefore, the parametrically generated second Stokes pulse is shortened according to the SRS depletion duration. This also gives us increased stability of the parametric Raman generation of the shortened pulse due to higher stability of the SRS depletion stage in comparison with all the process of the SRS generation of the first Stokes component.

The basic requirement on the parametric Raman generation of the second Stokes or first anti-Stokes component is the fulfillment of the phase matching condition of four-wave mixing involving the convertible fundamental laser

✉ M. Jelínek
michal.jelinek@fjfi.cvut.cz

¹ A.M. Prokhorov General Physics Institute of RAS, Vavilov Str. 38, Moscow, Russia 119991

² National University of Science and Technology MISiS, Leninskiy Prospekt 4, Moscow, Russia 119049

³ Faculty of Nuclear Sciences and Physical Engineering, Czech Technical University in Prague, Břehová 7, Prague, Czech Republic

radiation and the SRS-converted first Stokes component. Earlier, this phase matching condition was maintained in the non-collinear scheme using the laser pumping tilted with respect to the external cavity parametric Raman laser axis [10–12]. In our proposed method, we use the fulfillment of collinear phase matching of four-wave mixing of the orthogonally polarized Raman laser components in the certain direction inside the birefringent active Raman crystal [13] in the internal cavity Raman laser scheme.

In this paper, we demonstrate the effect of pulse shortening down to 300 ps of the parametrically generated radiation with the increased pulse energy under higher-power laser diode pumping of the miniature passively Q-switched Nd:SrMoO₄ parametric self-Raman laser and carry out the theoretical study and mathematical modeling of this effect.

2 Experimental study

Figure 1 shows the optical scheme of the diode-pumped Nd:SrMoO₄ parametric self-Raman laser. The laser system consists of the diode pump source, focusing optics, active 3-mm-long 0.7 at.% *a*-cut Nd:SrMoO₄ element (absorption coefficient at the pumping wavelength of 3.5 cm⁻¹, high-reflection coated on the input face and anti-reflection coated on the other face), anti-reflection-coated 5-mm-long Cr:YAG Q-switch with 80 % initial transmittance, and concave output coupler having high reflectivity of $R_{1.05-1.17} > 99\%$ for the fundamental ($\lambda_L = 1056$ nm) and first Stokes ($\lambda_S = 1165$ nm) components, and low reflectivity of $R_{1.30} = 20\%$ for the second Stokes component ($\lambda_{S2} = 1300$ nm). In order to increase the fundamental laser radiation intensity to overcome the SRS threshold, the laser cavity length was shortened to minimum corresponding to the closest position of the laser optical elements inside the cavity with the geometrical length of 1 cm (corresponding to the cavity optical length of 1.7 cm).

Because of low output coupler reflectivity at the second Stokes wavelength, the generation of the second Stokes component can be only parametrical [9]. The phase matching condition for the four-wave mixing

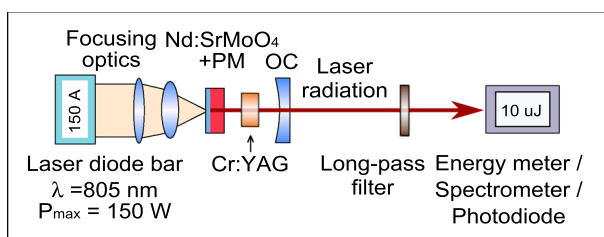


Fig. 1 Nd:SrMoO₄ self-Raman laser system schematic. *PM* pumping mirror, *OC* output coupler

($\lambda_{S2}^{-1} = \lambda_S^{-1} + \lambda_S^{-1} - \lambda_L^{-1}$) of the convertible fundamental laser radiation (λ_L) with the SRS-converted first Stokes component (λ_S) and the parametrically generated second Stokes component (λ_{S2}) has to be fulfilled. As it was shown in our previous work [9], this phase matching has a minimal mismatch of $\Delta k = 10$ cm⁻¹ for the *a*-cut Nd:SrMoO₄ crystal at the ooe-type interaction (the fundamental laser component is an ordinary wave, the first Stokes component is both ordinary and extraordinary, and the second Stokes component is an extraordinary wave) providing the operation around the 90°-angle phase matching insensitive to the angular mismatch if the crystal length L is short enough for the coherence condition [9] $\Delta k \cdot L < \pi$. And therefore we chose the short length of the *a*-cut Nd:SrMoO₄ crystal of $L = 3$ mm.

To increase the output energy of the Nd:SrMoO₄ parametric self-Raman laser, we used the pulsed high-power laser diode bar JOLD-808-QPFN (fast-axis collimation in the vertical plane) generating the peak power of 150 W (pulse duration 100 μs, repetition rate 10 Hz). This pump peak power was 7 times higher than in our previous work [9]. We also used the pump beam focusing in horizontal plane by two cylindrical lenses ($f_1 = 50$ and $f_2 = 12$ mm) into the spot of 1.3×2.9 mm² (horizontally oriented ellipse) at the Nd:SrMoO₄ crystal face. The laser diode output wavelength was stabilized at 805 nm close to the Nd:SrMoO₄ absorption peak. The linear polarization of the pump radiation was parallel to the optical axis of the active Nd:SrMoO₄ crystal (the same as in [9]).

Concave mirrors with the curvature radii of 0.5, 1, and 10 m, and also a plane mirror with reflectivity of $R_{1.05-1.17} = 99\%$ and $R_{1.30} = 20\%$ were used as output couplers.

The best output characteristics were obtained using the output coupler having the curvature radius of 10 m because of the best spatial overlap between the pumping and fundamental laser beam achievable using available mirrors. The pulse energies for the fundamental (1056 nm) laser radiation and the first Stokes (1165 nm) Raman component were as high as 8 and 56 μJ, respectively. The pulse energy for the parametrically generated second Stokes (1300 nm) Raman component exceeded 1 μJ (5 times higher than in [9]) and the pulse duration was 300 ps being approximately 10 times shorter than the first Stokes component. The second Stokes component polarization was vertical while the fundamental and the first Stokes waves were mainly horizontally polarized (with 10 % depolarization) confirming the second Stokes generation mechanism as parametric four-wave mixing of orthogonally polarized waves.

Figure 2 demonstrates the oscillogram of the Nd:SrMoO₄ laser output radiation measured by three InGaAs photodiodes EOT ET 3500 (analog bandwidth > 12.5 GHz, rise

time <35 ps) connected to a four-channel oscilloscope LeCroy SDA 9000 (analog bandwidth 6 GHz per channel) using coaxial cables of the same length with equal distances from the laser to the photodiodes. Figure 2 shows the second Stokes pulse is generated in the temporal region of overlapping the fundamental laser and the first Stokes pulses. This can be explained by four-wave mixing mechanism of the second Stokes generation with the strongest nonlinear cavity dumping pulse shortening because of depletion of the fundamental radiation terminating the second Stokes pulse generated by four-wave-mixing.

3 Theoretical study

The proposed pulse shortening method is based on the application of depletion of the fundamental laser radiation pulse due to the SRS conversion into the Stokes Raman component. Therefore, it is necessary to start our theoretical consideration from the well-known coupled wave equations for single-pass steady-state SRS taking into account the depletion of pumping [14]:

$$\begin{aligned} \frac{dI_L}{dz} &= -g_R \cdot \frac{\lambda_S}{\lambda_L} \cdot I_S \cdot I_L, \\ \frac{dI_S}{dz} &= g_R \cdot I_L \cdot I_S, \end{aligned} \quad (1)$$

where I_L and I_S are the intensities of the laser (pumping) and SRS (first Stokes) radiation, λ_L and λ_S are its wavelengths, g_R is the Raman gain (in cm/W) distributed over the interaction length L_R . The analytical solution of (1) in the case of undepleted pumping is also well known [14]: $I_S(z) = I_S(0) \cdot \exp(g_R \cdot I_L \cdot z)$. The analytical solution taking into account the depletion of pumping was derived too (for example, see [15]), but early it did not attract any attention. This solution can be written as

$$\begin{aligned} I_L(z) &= I_0 - \frac{\lambda_S}{\lambda_L} \cdot I_S(z) \approx I_L(0) - \frac{\lambda_S}{\lambda_L} \cdot I_S(z), \\ I_S(z) &= \frac{I_0}{\frac{\lambda_S}{\lambda_L} + \frac{I_L(0)}{I_S(0)} \cdot e^{-g_R \cdot I_0 \cdot z}} \approx \frac{I_L(0)}{\frac{\lambda_S}{\lambda_L} + \frac{I_L(0)}{I_S(0)} \cdot e^{-g_R \cdot I_L(0) \cdot z}}, \end{aligned} \quad (2)$$

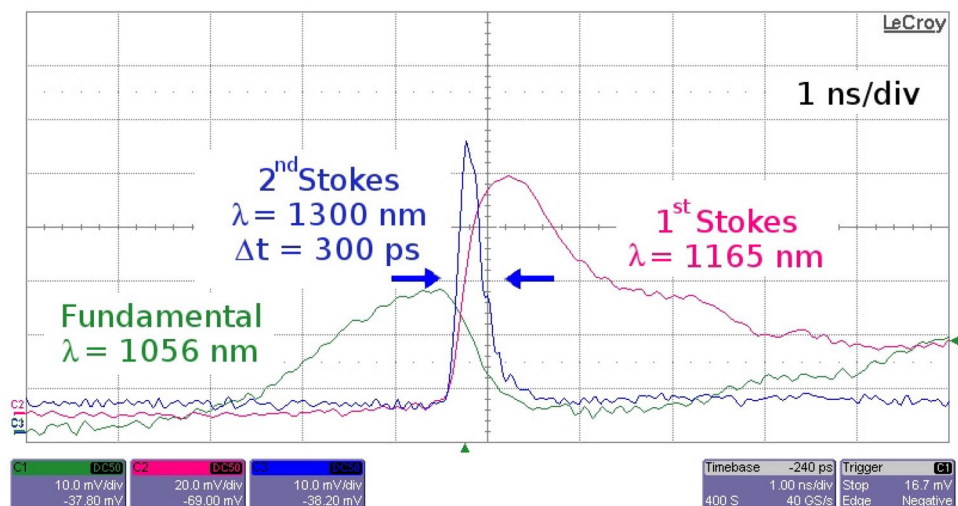
where $I_L(0)$ and $I_S(0)$ are the intensities of the interacting radiation components at the SRS medium input ($z = 0$), $I_0 = I_L(0) + I_S(0) \cdot \lambda_S/\lambda_L$. The approximate equality in (2) is valid when $I_S(0) \ll I_L(0)$ and corresponds to the case of the SRS generation that is important for us here. Then as a result of SRS generation with full depletion of pumping ($I_L(z) \rightarrow 0$) the Stokes SRS component grows up to its limit value of $I_S^\infty \cong I_L(0) \cdot \lambda_L/\lambda_S$ that follows from the law of energy conservation $I_L(z) + I_S(z) \cdot \lambda_S/\lambda_L \cong I_L(0)$. The fastest changes in the intensities $I_L(z)$ and $I_S(z)$ take place at the short region of SRS depletion of pumping. We can determine the region of SRS depletion of pumping as the distance of decreasing the pumping laser intensity from $I_L(z_1) = 0.9I_L(0)$ down to $I_L(z_2) = 0.1I_L(0)$; then, $\Delta z = z_2 - z_1$ is the spatial extension of the region of SRS depletion of the pumping laser radiation. The same region can also be determined as the distance of the increasing Stokes SRS radiation intensity from $I_S(z_1) = 0.1I_S^\infty$ up to $I_S(z_2) = 0.9I_S^\infty$. According to (2), the spatial extension of the region of SRS depletion of pumping laser radiation is

$$\Delta z = \frac{\ln(0.9/0.1)^2}{g_R \cdot I_L(0)} \approx \frac{4.4}{g_R \cdot I_L(0)}. \quad (3)$$

It can be seen that the region Δz is inversely proportional to the pumping laser radiation intensity and the Raman gain.

Depletion of pumping of the single-pass SRS determined by the solving (2) is a purely spatial effect and cannot give the radiation temporal shape control. At the single-pass process, it is correct not only for the steady-state case (continuous wave pumping), but also for a quasi-steady-state

Fig. 2 Oscillogram of the diode-pumped Nd:SrMoO₄ self-Raman laser (1 ns/div.): (C1—green) the fundamental laser radiation, (C2—magenta) the first Stokes component, (C3—blue) the second Stokes Raman component



SRS with pumping pulse duration essentially higher than the vibrational dephasing time of the SRS medium. In the case of a transient single-pass SRS, the possibility of the radiation temporal shape control appears owing to delay of generating SRS pulse because the transient SRS gain depends on the pumping energy density and not the pumping intensity [16] in contrast to the previous cases.

The situation with depletion of pumping can be changed in a case of intracavity SRS. Depletion of pumping becomes not only the spatial effect but also a temporal effect even for the quasi-steady-state SRS. It gives us the possibility to apply depletion of pumping for pulse shortening of the intracavity parametric Raman laser radiation.

The aim of application of an optical cavity for the SRS medium is usually decreasing the required (threshold) intensity of pumping because of increasing an effective length of SRS interaction by multipass SRS generation. The SRS interaction effective length can be defined as $L_{\text{eff}} = L \cdot N_{\text{eff}}$, where L is the SRS medium length, N_{eff} is the effective number of passes of SRS radiation through the optical cavity of the SRS medium. Therefore, the SRS generation in such SRS laser appears after many passes of the SRS radiation through the cavity. It leads to a delay of the generated SRS pulse in time, and therefore, SRS depletion of pumping takes place now not only in space, but also in time. Then in the case of full depletion of pumping we can get the shortest duration of the stage of depletion of pumping

$$\Delta t = \frac{\Delta z}{c} \approx \frac{4.4}{g_R \cdot I_L \cdot c}, \tag{4}$$

where c is the speed of light in vacuum, $g_R = g \cdot L/L_R$ is the Raman gain distributed over the cavity length, g is the Raman gain of the SRS medium, L_R is the cavity optical length, I_L is the intensity of undepleted laser pumping in the SRS medium.

The SRS generation threshold can be defined by the well-known condition [17]

$$g \cdot I_L^{\text{th}} \cdot L_{\text{eff}} \approx 25, \tag{5}$$

where I_L^{th} is the threshold intensity of pumping in the SRS medium. On the other hand, for the SRS laser cavity fully occupied by the SRS medium this condition can be written as [8]

$$(g_R \cdot I_L^{\text{th}} - k_R) \cdot \tau_L \cdot c \approx 25, \tag{6}$$

where k_R is the cavity loss coefficient distributed over the cavity length, τ_L is the laser pumping pulse duration, $\tau_L \cdot c$ is the spatial length of the laser pumping pulse. Taking into account $g_R = g \cdot L/L_R$, $L_{\text{eff}} = L \cdot N_{\text{eff}}$, and

$k_R = L_R^{-1} \cdot \ln \left(1 / \left(T_s \cdot \sqrt{R_S^{\text{in}} \cdot R_S^{\text{out}}} \right) \right)$, where T_S is the intracavity medium single-pass transmittance for the SRS radiation (giving the intracavity losses), R_S^{in} and R_S^{out} are the reflectivities of the cavity input and output mirrors for the SRS radiation, respectively; from (5) and (6) we obtain [8]

$$N_{\text{eff}} = \left(\frac{\tau_R}{\tau_L} + \frac{1}{25} \cdot \ln \frac{1}{T_S \cdot \sqrt{R_S^{\text{in}} \cdot R_S^{\text{out}}}} \right)^{-1}, \tag{7}$$

where $\tau_R = L_R/c$ is the cavity transit time. Consequently the threshold intensity of the single-pass pumping is

$$I_L^{\text{th}} = \frac{25}{g \cdot L} \cdot \left(\frac{\tau_R}{\tau_L} + \frac{1}{25} \cdot \ln \frac{1}{T_S \cdot \sqrt{R_S^{\text{in}} \cdot R_S^{\text{out}}}} \right). \tag{8}$$

Then the generating SRS pulse delay t_S is equal to the pumping pulse duration τ_L . Overcoming the SRS generation threshold the generating SRS pulse delay decreases lower than the pumping pulse duration. We can determine the delay t_S replacing τ_L by t_S and I_L^{th} by I_L in the condition (6), then [18]

$$t_S = \frac{25 \cdot \tau_R}{g \cdot I_L \cdot L + \ln \left(T_S \cdot \sqrt{R_S^{\text{in}} \cdot R_S^{\text{out}}} \right)}. \tag{9}$$

If $t_S > \tau_L$ we get $I_L < I_L^{\text{th}}$, then the SRS generation does not occur.

In the case of the external cavity Raman laser, the pumping is usually carried out by the single pass through the SRS medium, and so depletion of pumping increases in the SRS medium from its input to its output. Therefore, at the SRS medium input we necessarily have the undepleted pump radiation intensity, and only at the SRS medium output we can get full depletion of pumping with the shortest duration Δt determined by (4). However, for our method of generating pulse shortening to the value close to Δt we have to get over this problem of spatially non-uniform intensity of laser pumping $I_L(z)$ determined by (2). Otherwise the presence of the undepleted pump radiation at the input part of the SRS medium will prevent termination of the parametric generation, and therefore, the parametrically generated pulse would not be shortened. Using the double-pass pumping for the external cavity Raman laser (when the cavity output mirror reflects the pump radiation) results in decreasing the spatially non-uniform depletion of pumping, but do not solve the problem because at the SRS medium input we again have the undepleted pump radiation. The solution lies in using the intracavity pumping of the Raman laser (the internal cavity Raman laser) only where the reflection of not only the SRS

radiation but also the pump radiation from the cavity mirrors results in the multipass pumping with the best spatially uniform depletion of pumping.

For the first time, the pulse shortening of the parametrically generated second Stokes radiation component of the parametric Raman laser was demonstrated in [19] at the intracavity pumping of the calcite SRS crystal by the second harmonic (532 nm) neodymium laser utilizing the second harmonic generation inside the SRS crystal optical cavity. At the certain angle of incidence on the calcite SRS crystal corresponding to the phase matching of parametric four-wave mixing, the low-threshold parametric generation of the second Stokes component took place with shorter pulse duration (4 ns) than for the first Stokes component (8 ns). The pulse shortening was not so significant (by 2 times) because of the high-Q cavity for all the interacting components in the parametric Raman laser, and so the parametrically generated second Stokes pulse duration was close to the photon lifetime in the cavity of about 4 ns.

For the strongest shortening of the generating pulse, it is necessary to use the output mirror with high transmittance at the wavelength of the parametrically generated radiation component, and then, its pulse duration can be shortened close to the duration of the stage of the pump depletion Δt . For the first time, it was realized by our group in [9] and demonstrated here (see Fig. 2) with higher output energy in the diode-pumped, passively Q-switched Nd:SrMoO₄ parametric self-Raman laser (see Fig. 1).

The shortened pulse duration can be estimated according to the duration of the stage of pump depletion Δt (4) where it is necessary to define the intracavity intensity of the convertible fundamental laser radiation I_L . The lasing parameters in the passively Q-switched regime can be calculated according to the formulas [8]

$$I_L \approx c \cdot k_0 \cdot U_L^{\text{sat}} \cdot \left[1 - \frac{k_1}{k_0} \cdot \left(1 + \ln \frac{k_0}{k_1} \right) \right], \tag{10}$$

$$\tau_L \approx \frac{1}{c \cdot k_1 \cdot \left[1 - \frac{k_1}{k_0} \cdot \left(1 + \ln \frac{k_0}{k_1} \right) \right]}, \tag{11}$$

where U_L^{sat} is the gain saturation energy density for the active laser crystal,

$$k_{0,1} = \frac{1}{L_R} \cdot \ln \frac{1}{T_{0,1} \cdot \sqrt{R_L^{\text{in}} \cdot R_L^{\text{out}}}}, \tag{12}$$

are the cavity loss coefficients in the case of unsaturated and saturated passive Q-switch, respectively; T_0 and T_1 are the Q-switch transmittances in the unsaturated and saturated states; L_R is the cavity optical length; R_L^{in} and R_L^{out} are the cavity input and output mirrors reflectivities at the fundamental laser radiation wavelength. So, at the input parameters used in the

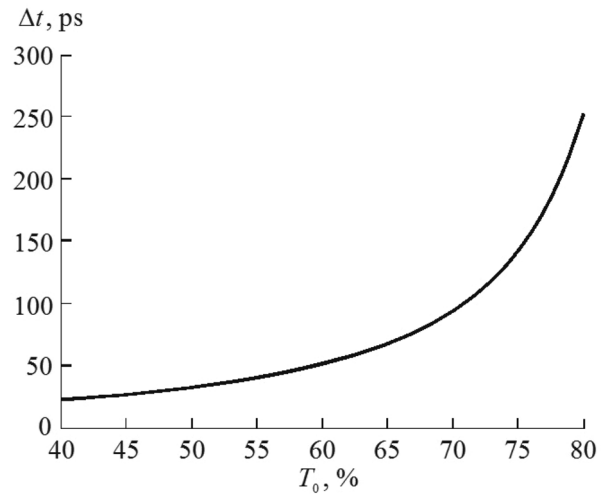


Fig. 3 Theoretical dependence of the estimated duration Δt of the shortened parametrically generated pulse of the passively Q-switched Nd:SrMoO₄ parametric self-Raman laser on the initial transmittance T_0 of the passive Q-switch at the same other input parameters: $T_1 = 92 \%$, $R_{L1} = R_{L2} = 99 \%$, $U_L^{\text{sat}} = 0.62 \text{ J/cm}^2$, $g = 5.7 \text{ cm/GW}$, and $L_R = 2.5 \text{ cm}$

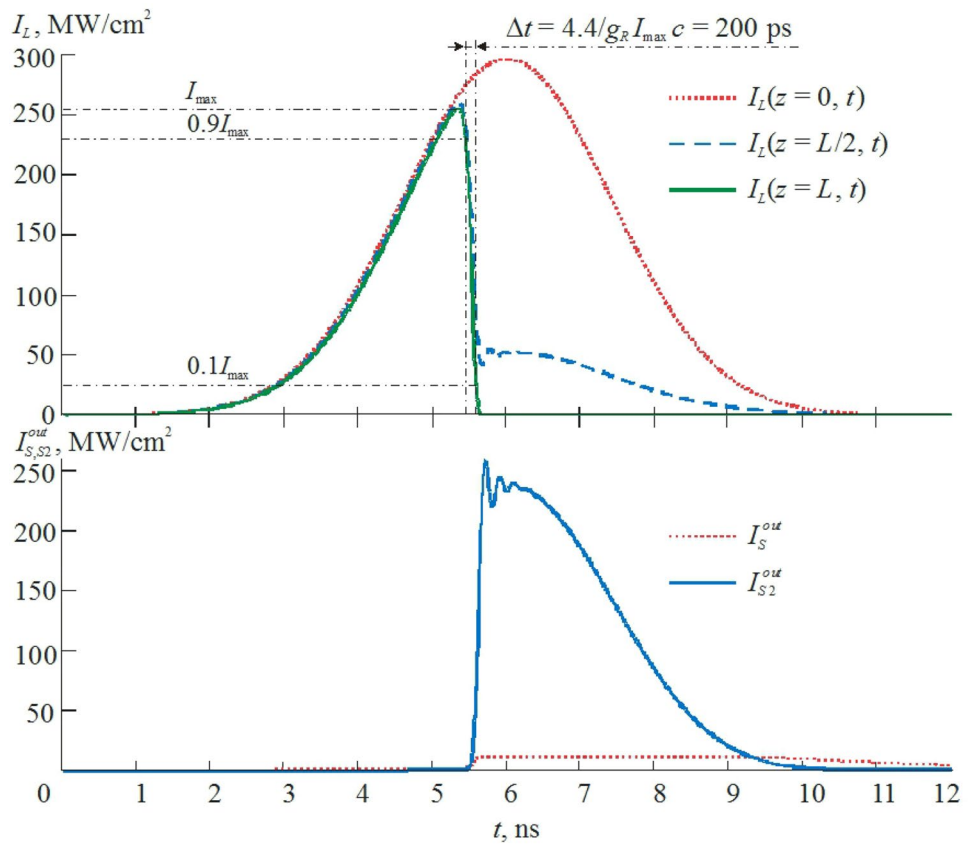
experiment [9] were: $T_0 = 80, T_1 = 92, R_L^{\text{in}} = R_L^{\text{out}} = 99 \%$, $U_L^{\text{sat}} = h \cdot \nu_L / \sigma_{\text{em}} = 0.62 \text{ J/cm}^2$, $\sigma_{\text{em}} = 3 \cdot 10^{-19} \text{ cm}^2$, $L = 0.3 \text{ cm}$, and $L_R = 1.7 \text{ cm}$. From (10)–(12), we obtain $I_L \approx 600 \text{ MW/cm}^2$ and $\tau_L = 4.2 \text{ ns}$. Then the shortened pulse duration of the parametrically generated second Stokes component estimated as Δt (4) amounts 250 ps assuming $g = 5.7 \text{ cm/GW}$ for the SrMoO₄ crystal [8] being in agreement with the experimental value of 280–300 ps, but the experimental value is slightly higher that can be explained by non-ideal pulse shortening and should be studied by the mathematical modeling.

Figure 3 shows the theoretical dependence of the estimated duration Δt of the shortened parametrically generated pulse of the passively Q-switched Nd:SrMoO₄ parametric self-Raman laser on the initial transmittance T_0 of the passive Q-switch calculated according to (4), (10), and (12) at the same other input parameters (except T_0). It can be seen that decreasing the initial transmittance of the passive Q-switch 2 times from 80 to 40 % leads to fast shortening (10 times) of the estimated duration Δt of the shortened parametrically generated pulse from 250 ps down to 22 ps, and so using the optically denser passive Q-switches can help to get single or repetitive ultrashort picosecond pulses without any mode-locking device.

4 Mathematical modeling

To study features of the pulse shortening we carried out the mathematical modeling of generation in the parametric

Fig. 4 Numerical simulation results for the external cavity parametric Raman laser with single-pass pumping of the SrMoO₄ SRS crystal with the length $L = 1$ cm at the output mirror reflectance $R_S^{\text{out}} = 0.95$ in the case of the pump laser pulse of Gaussian shape with duration of $\tau_L = 4$ ns and peak intensity of $I_L^{\text{in}} = 297$ MW/cm²



Raman laser cavity under laser pumping by nanosecond pulses. We supposed that the birefringent SRS crystal is cut in phase-matched direction for four-wave mixing of the fundamental laser radiation (pumping) with its first and second Stokes Raman components, and the cavity mirrors are placed directly at the faces of the SRS crystal (the laser cavity is fully occupied by the SRS medium). The intracavity losses can be neglected here ($T_S = 1$). For the modeling, we used the coupled wave rate equations [18]:

$$\begin{aligned}
 &\pm \frac{\partial E_L^{(\pm)}}{\partial z} + \frac{n}{c} \cdot \frac{\partial E_L^{(\pm)}}{\partial t} = -\frac{g}{2} \cdot \frac{\lambda_S}{\lambda_L} \cdot \left(|E_S^{(+)}|^2 + |E_S^{(-)}|^2 \right) \\
 &\quad \cdot E_L^{(\pm)} - \frac{g}{2} \cdot \frac{\lambda_S}{\lambda_L} \cdot \left(E_S^{(\pm)} \right)^2 \cdot E_{S2}^{*(\pm)}, \\
 &\pm \frac{\partial E_S^{(\pm)}}{\partial z} + \frac{n}{c} \cdot \frac{\partial E_S^{(\pm)}}{\partial t} = \frac{g}{2} \cdot \left(|E_L^{(+)}|^2 + |E_L^{(-)}|^2 \right) \\
 &\quad \cdot E_S^{(\pm)} - \frac{g}{2} \cdot \frac{\lambda_{S2}}{\lambda_S} \cdot \left(|E_{S2}^{(+)}|^2 + |E_{S2}^{(-)}|^2 \right) \cdot E_S^{(\pm)}, \\
 &\pm \frac{\partial E_{S2}^{(\pm)}}{\partial z} + \frac{n}{c} \cdot \frac{\partial E_{S2}^{(\pm)}}{\partial t} = \frac{g}{2} \cdot \left(|E_S^{(+)}|^2 + |E_S^{(-)}|^2 \right) \\
 &\quad \cdot E_{S2}^{(\pm)} + \frac{g}{2} \cdot \left(E_S^{(\pm)} \right)^2 \cdot E_L^{*(\pm)},
 \end{aligned}
 \tag{13}$$

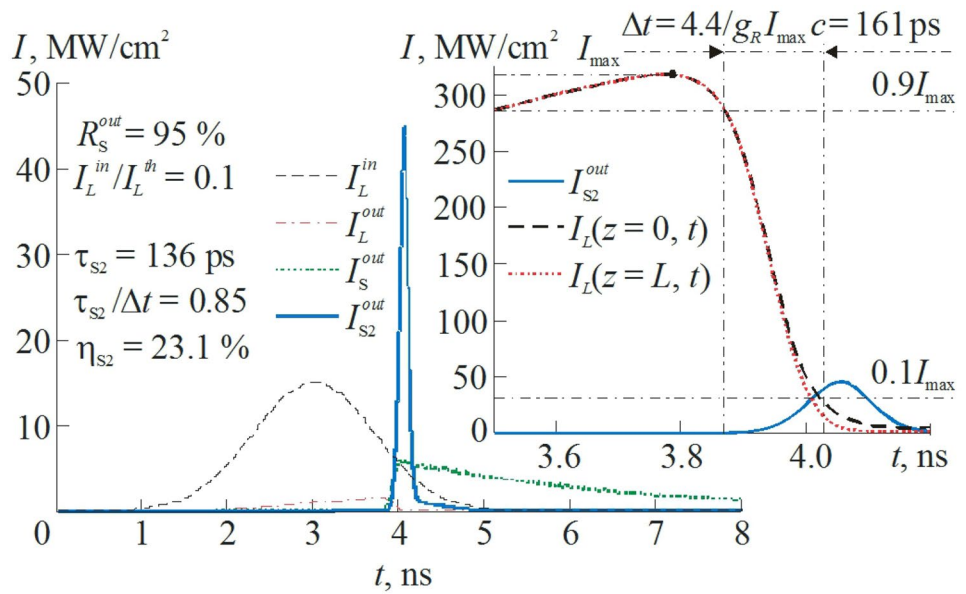
where n is the refractive index of the SRS medium, $E_L^{(\pm)}$, $E_S^{(\pm)}$, and $E_{S2}^{(\pm)}$ are the slowly varying complex amplitudes of the fundamental, first Stokes, and second Stokes radiation components propagating in forward (+) and backward (-) directions; λ_L , λ_S , and λ_{S2} are wavelengths. The sum $\left(|E_{L,S,S2}^{(+)}|^2 + |E_{L,S,S2}^{(-)}|^2 \right)$ in (13) means the SRS interaction of not only waves propagating in one direction, but counter-propagating waves in the laser cavity. The last terms in the first and last equations of the system (13) describe the parametric coupling under phase matching condition for waves propagating in one direction.

For the external cavity parametric Raman laser, the boundary conditions can be written as

$$\begin{aligned}
 E_L^{(+)}(0, t) &= \sqrt{I_L^{\text{in}}(t)}, \\
 E_{S,S2}^{(+)}(0, t) &= E_{S,S2}^{(-)}(0, t), \\
 E_{L,S,S2}^{(-)}(L, t) &= E_{L,S,S2}^{(+)}(L, t) \cdot \sqrt{R_{L,S,S2}^{\text{out}}},
 \end{aligned}
 \tag{14}$$

where $R_{L,S,S2}^{\text{in,out}}$ is the reflectance of the cavity input (in) and output (out) mirrors for the respective radiation components, $I_L^{\text{in}}(t)$ is the temporal dependence of the pump laser pulse intensity at the SRS medium input. In (14), there is

Fig. 5 Result of numerical simulation for the same parametric Raman laser but with $R_L^{in} = 1$ and $R_L^{out} = 0.99$ at the intracavity pumping by the Gaussian pulse with duration of $\tau_L = 2$ ns and peak intensity of $I_L^{in} = 15$ MW/cm²



taken into account that $R_L^{in} = 0$ and $R_{S,S2}^{in} = 1$. To prevent the second Stokes cascade-like SRS generation in order to realize purely its parametric generation, we consider $R_{S2}^{out} = 0$.

Figure 4 shows the result of the numerical solution of the system (13) with the boundary condition (14) for the SrMoO₄ SRS crystal with the Raman gain $g = 5.7$ cm/GW, the length $L = 1$ cm, and the refractive index $n = 2$ corresponding to the cavity single-pass transit time $\tau_R = L \cdot n/c = 66.6$ ps at the output mirror reflectivity $R_L^{out} = 0$ (single-pass pumping) and $R_S^{out} = 0.95$ in the case of the pump laser pulse $I_L^{in}(t)$ of Gaussian shape with the duration $\tau_L = 4$ ns at the 1/e level. The delay of the SRS generation pulse t_S (9) is assigned here $t_S = \tau_L/4 = 1$ ns giving the peak intensity of the input pump laser pulse

$$I_L^{in} = \frac{25}{g \cdot L} \cdot \left(\frac{\tau_R}{t_S} + \frac{1}{25} \cdot \ln \frac{1}{T_S \cdot \sqrt{R_S^{in} \cdot R_S^{out}}} \right) = 297 \text{ MW/cm}^2$$

that is in 3.8 times higher than the threshold value (8) $I_L^{th} = 78$ MW/cm².

On the upper graph in Fig. 4, there is the depleted pump pulse at the SRS medium input ($z = 0$), middle ($z = L/2$), and output ($z = L$). Note that, full depletion of pumping with duration $\Delta t \approx 200$ ps (4) is observed only at the SRS medium output ($z = L$). At the SRS medium input ($z = 0$) the pump pulse is undepleted, but the depletion of pumping grows passing through the SRS medium (for example, $z = L/2$).

On the bottom graph the output pulses of the first and second Stokes SRS components are shown. As can be seen the pulse shortening of the parametrically generated second Stokes component did not happen that can be explained by

not full depletion of pumping resulting in the continued parametric generation to the end of the pump pulse.

The modeling results for the double-pass ($R_L^{out} = 1$) pumped external cavity parametric Raman laser were similar, but the spatially non-uniform depletion of pumping was lower. However, we again had the undepleted pump radiation at the SRS medium input, and therefore, the generation character did not change. But it is necessary to note that increasing the number of passes of the pump radiation through the SRS medium allows to decrease the spatially non-uniform depletion of pumping.

The highest number of passes of pumping can be achieved using the internal cavity Raman laser where not only the SRS radiation but also the fundamental (pumping for SRS) laser radiation is generating inside the SRS laser cavity. Generation of the fundamental laser radiation in the internal cavity SRS can be realized in the additional laser or nonlinear medium (for example, frequency doubler [19]) inside the same Raman laser cavity, or even directly in the self-Raman laser medium [9].

For the internal cavity parametric Raman laser, the boundary conditions can be rewritten as

$$\begin{aligned} E_L^{(+)}(0, t) &= \sqrt{I_L^{in}(t) + |E_L^{(-)}(0, t)|^2} \cdot R_L^{in}, \\ E_{S,S2}^{(+)}(0, t) &= E_{S,S2}^{(-)}(0, t), \\ E_{L,S,S2}^{(-)}(L, t) &= E_{L,S,S2}^{(+)}(L, t) \cdot \sqrt{R_{L,S,S2}^{out}}, \end{aligned} \tag{15}$$

where we took into account that the fundamental laser pulse $I_L^{in}(t)$ is generating inside the laser cavity at the SRS medium input. The process of the fundamental laser

generation is not considered here, but the generated fundamental (pump) laser pulse $I_L^{in}(t)$ with the peak intensity I_L^{in} and duration τ_L is assigned here as the input parameter of the calculation as before.

It is necessary to note that if the pump laser pulse duration τ_L is essentially higher than the cavity transit time τ_R , then the intracavity pump intensity I_L in the SRS medium is essentially higher than I_L^{in} due to the reflection from the cavity mirrors. For example, in the case of a rectangular pump pulse we have

$$I_L \approx I_L^{in} \cdot \sum_{n=1}^{N_L} \left[\left(R_L^{in} \cdot R_L^{out} \right)^n + \left(R_L^{in} \right)^n \cdot \left(R_L^{out} \right)^{n+1} \right] \quad (16)$$

where $N_L \approx \tau_L / 2\tau_R$ is an integer number of round trips of the fundamental laser radiation through the laser cavity during the laser pulse duration. From (16), at fully reflecting mirrors of the cavity we obtain the highest growth of the intracavity pump intensity I_L by τ_L / τ_R times in comparison with I_L^{in} . In the case of the Gaussian pump pulse and not fully reflecting mirrors this growth is lower, but in any case the intracavity pumping leads to decreasing the SRS generation threshold in comparison with the value I_L^{th} (8) obtained for the single-pass pumping.

Figure 5 demonstrates the numerical solution result of the system (13) with the boundary conditions (15) for the same parametric Raman laser but with $R_L^{in} = 1$ and $R_L^{out} = 0.99$ at the intracavity pumping by the Gaussian pulse with the duration of $\tau_L = 2$ ns at the 1/e level ($\tau_L / \tau_R = 30$) and peak intensity of $I_L^{in} = 15$ MW/cm² that is 10 times lower than the single-pass pump threshold value I_L^{th} (8).

Figure 5 shows that in spite of a low value of the input pump intensity I_L^{in} (compared with I_L^{th}) the second Stokes pulse (I_{S2}^{out}) shortening takes place now with the pulse duration of $\tau_{S2} = 136$ ps and high generation efficiency of $\eta_{S2} = 23.1$ %. The second Stokes pulse is 14.7 times shorter than τ_L .

High generation efficiency of the shortened second Stokes pulse is caused by high rate of its parametric generation close to the rate of the first Stokes SRS generation and also by high transmittance ($R_{S2}^{out} = 0$) of the cavity output mirror at the second Stokes wavelength resulting in the efficient nonlinear (parametric) cavity dumping.

In addition, in Fig. 5 together with the parametrically generated pulse (I_{S2}^{out}) there are shown the temporal dependences of the intracavity pump intensity at the SRS medium input and output $I_L(z = 0, t) = |E_L^{(+)}(z = 0, t)|^2 + |E_L^{(-)}(z = 0, t)|^2$ and $I_L(z = L, t) = |E_L^{(+)}(z = L, t)|^2 + |E_L^{(-)}(z = L, t)|^2$. It can be seen that not only at the SRS medium output but also at the SRS medium input there is practically full depletion

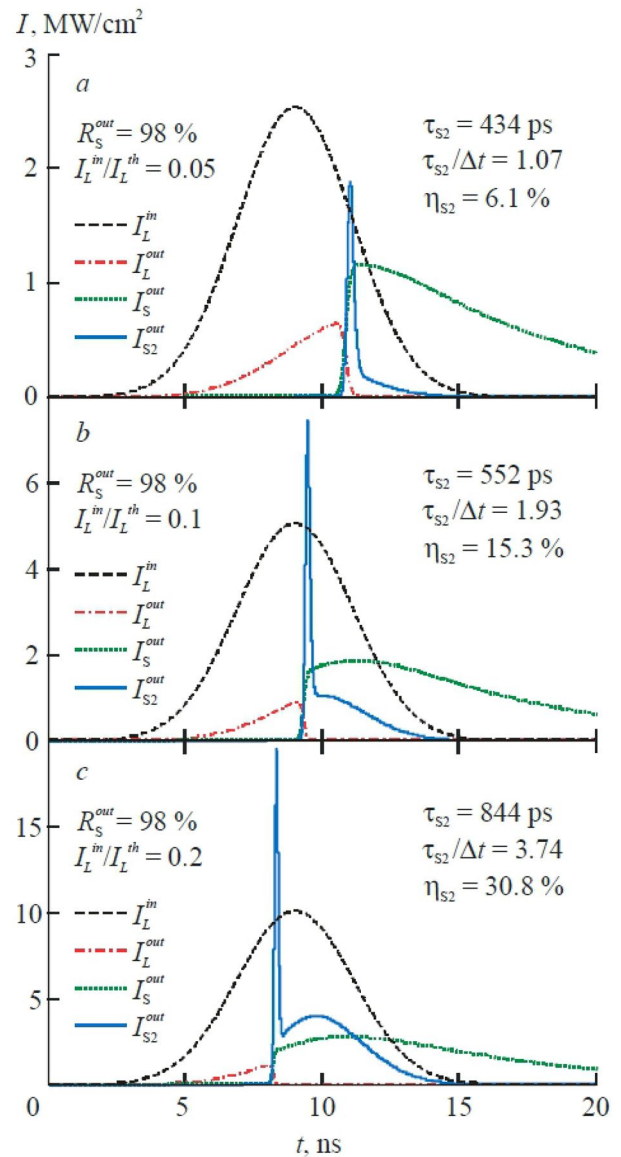


Fig. 6 Results of numerical simulation for the parametric Raman laser with the intracavity pumping by the Gaussian pulse with duration of $\tau_L = 4$ ns at $R_S^{out} = 0.98$ for various values of the pump level a $I_L^{in}/I_L^{th} = 0.05$, b $I_L^{in}/I_L^{th} = 0.1$ and c $I_L^{in}/I_L^{th} = 0.2$

of pumping with the short depletion stage duration Δt determined by formula (4), and so the intracavity pumping allowed to solve the problem of spatially non-uniform depletion of pumping. Therefore, the pulse shortening of the parametrically generated second Stokes component to the duration τ_{S2} close to Δt (4) took place.

Figure 6 shows the simulation results of generation of the same parametric Raman laser with intracavity pumping by the laser pulse with the duration of $\tau_L = 4$ ns at $R_S^{out} = 0.98$ for various values of the input pump pulse intensity $I_L^{in}/I_L^{th} = 0.05, 0.1$, and 0.2 (the values normalized to the single-pass pumping threshold intensity I_L^{th} (8)).

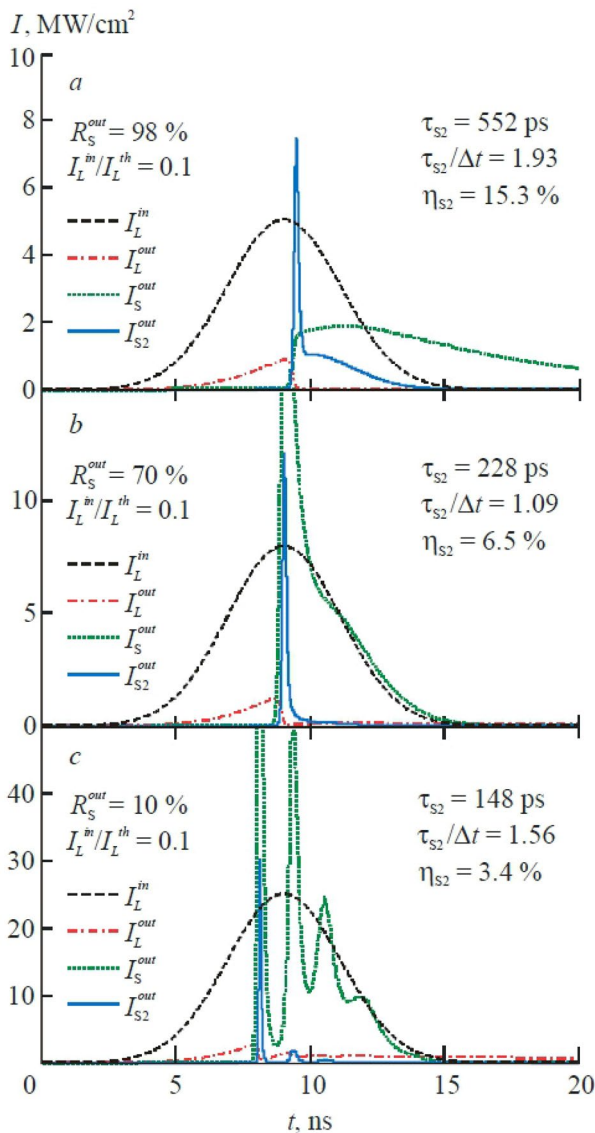


Fig. 7 Results of numerical simulation for the parametric Raman laser with the intracavity pumping by the Gaussian pulse with duration of $\tau_L = 4$ ns at the pump level $I_L^{in}/I_L^{th} = 0.1$ and various values of the cavity output mirror at the first Stokes wavelength: **a** $R_S^{out} = 0.98$, **b** $R_S^{out} = 0.70$, and **c** $R_S^{out} = 0.10$

Figure 6 shows that at the twice longer pump pulse duration (than in the previous case) qualitative shortening of the parametrically generated pulse only under halved pump level $I_L^{in}/I_L^{th} = 0.05$ can be achieved (Fig. 6a). Therefore, the pulse duration is longer due to slower depletion of pumping (Δt (4)). The quality of pulse shortening can be defined by the parameter $\tau_{S2}/\Delta t$ which amounts 1.07 in the case of Fig. 6a that is close to the ideal case $\tau_{S2}/\Delta t = 1$.

Increasing the pump level resulted in the pulse shortening quality decrease: $\tau_{S2}/\Delta t$ is increased up to 1.93 at $I_L^{in}/I_L^{th} = 0.1$ (Fig. 6b) and up to 3.74 at $I_L^{in}/I_L^{th} = 0.2$ (Fig. 6c). Therefore, in spite of decreasing Δt (4) with

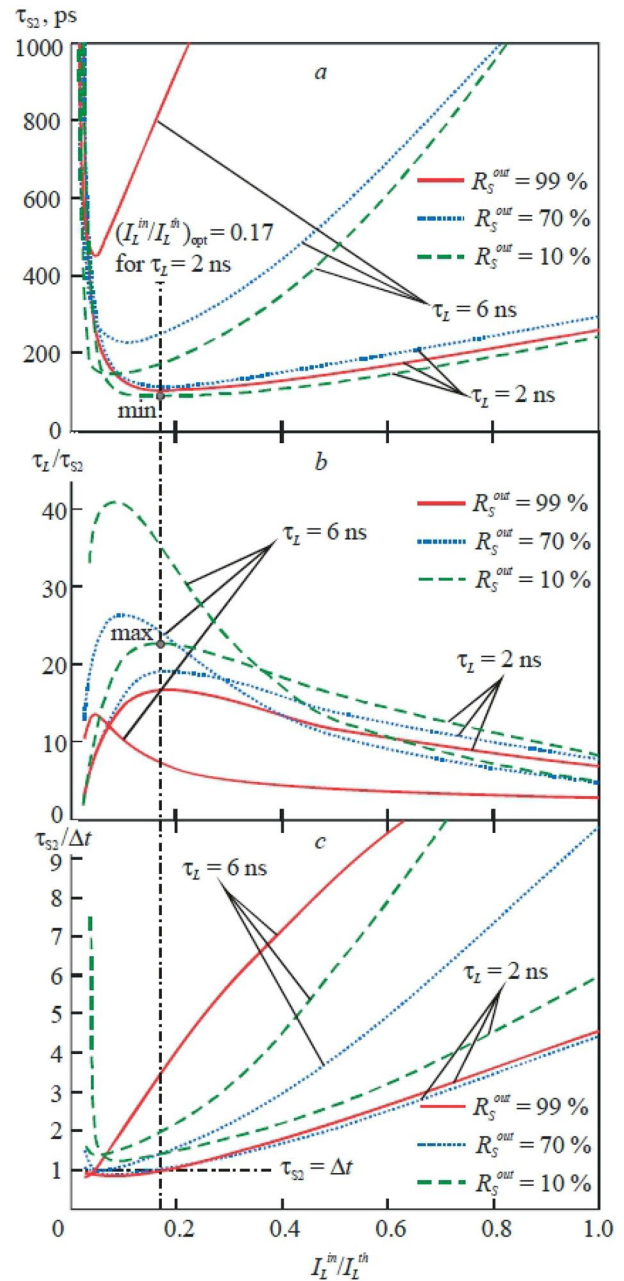


Fig. 8 Calculated dependences of: **a** the parametrically generated pulse duration τ_{S2} , **b** the pulse shortening relative value τ_L/τ_{S2} , and **c** the quality of pulse shortening $\tau_{S2}/\Delta t$ on the pump level I_L^{in}/I_L^{th} at the pump pulse durations of $\tau_L = 2$ ns and $\tau_L = 6$ ns for the cavity output mirror reflectivity at the first Stokes wavelength of $R_S^{out} = 0.99$, 0.70, and 0.10

increasing the pump intensity the absolute value of the shortened pulse duration increased to 552 ps (Fig. 6b) and 844 ps (Fig. 6c), respectively. Figure 6 shows that the decrease in the pulse shortening quality is caused by the fact that after the shortened pulse the long trailing edge (post-pulse) appears with a shape close to the pump pulse shape.

It is necessary to note that at longer pump pulse ($\tau_L = 4$ ns) than in the previous case ($\tau_L = 2$ ns) the pulse shortening quality decrease appears at lower I_L^{in}/I_L^{th} , and so the generation efficiency of the qualitatively shortened pulse here is lower and amounts only $\eta_{S2} = 6.1\%$ (Fig. 6a) in comparison with 23.1 % (Fig. 5). Consequently the increased pump pulse duration ($\tau_L = 4$ ns) is non-optimal for efficient parametric generation of the shortened pulse in contrast to the previous case ($\tau_L = 2$ ns).

In the works [4–6], it was shown that decreasing the cavity output mirror reflectivity at the first Stokes wavelength led to the pulse shortening of the first Stokes SRS generation. It is caused by the nonlinear cavity dumping owing to the SRS frequency conversion [8]. In the present work, we study the second Stokes pulse shortening via nonlinear cavity dumping owing to the parametric frequency conversion. It is also interesting to study the nonlinear cavity dumping owing to both the SRS ($R_S^{out} < R_L^{out}$) and parametric ($R_{S2}^{out} = 0$) frequency conversions.

Figure 7 demonstrates the simulation results for the same parametric Raman laser with intracavity pumping by the laser pulse with duration of $\tau_L = 4$ ns at the pump level $I_L^{in}/I_L^{th} = 0.1$ and various values of the cavity output mirror at the first Stokes wavelength $R_S^{out} = 0.98, 0.70$, and 0.10.

Figure 7 shows that decreasing the cavity output mirror reflectivity R_S^{out} at the first Stokes wavelength resulted in more significant pulse shortening of the parametrically generated second Stokes component. Firstly it is caused by increasing the threshold value I_L^{th} (8) with decreasing R_S^{out} that leads to a proportional increase in the input pump pulse intensity I_L^{in} corresponding to the given pump level $I_L^{in}/I_L^{th} = 0.1$; therefore, the duration Δt (4) of the pumping depletion stage shortens with increasing the pump intensity, and so the second Stokes pulse shortens too. Secondly the long post-pulse of the second Stokes shortened pulse disappears because of the SRS dumping of the cavity resulting in the pulse shortening of the first Stokes SRS generation; therefore, the quality of the pulse shortening ($\tau_{S2}/\Delta t$) of the parametrically generated second Stokes component is improved. So, at $R_S^{out} = 0.70$ (Fig. 7b) the pulse shortening quality is close to ideal ($\tau_{S2}/\Delta t = 1.09$), and the generation efficiency of $\eta_{S2} = 6.5\%$ is higher than for the most shortened pulse in Fig. 6 ($\eta_{S2} = 6.1\%$ at $\tau_{S2}/\Delta t = 1.07$ in Fig. 6a), and also the absolute value of the parametrically generated pulse duration is halved.

At further decreasing R_S^{out} down to 10 % (Fig. 7c), the second Stokes pulse is shortened still more by 1.5 times to 148 ps at the pulse shortening relative value of $\tau_L/\tau_{S2} = 27$, but the quality of the pulse shortening rather decreased ($\tau_{S2}/\Delta t = 1.56$) that is caused by oscillations of the generated Raman components due to too fast SRS dumping of the cavity. The shortened pulse generation efficiency decreased to $\eta_{S2} = 3.4\%$.

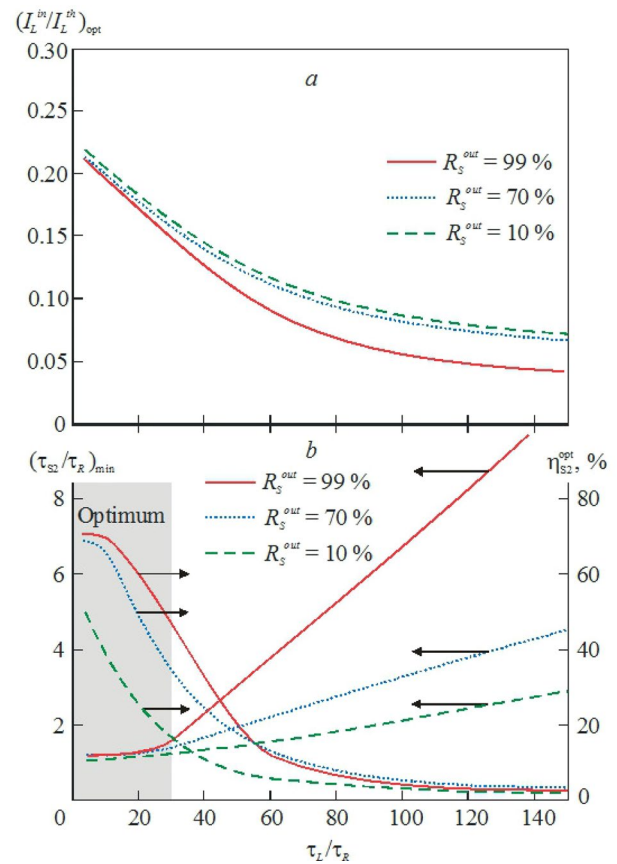


Fig. 9 Calculated dependences of: **a** the optimum pump level $(I_L^{in}/I_L^{th})_{opt}$, **b** the minimum generated pulse duration $(\tau_{S2}/\tau_R)_{min}$, and the generation efficiency η_{S2}^{opt} of the second Stokes pulse with minimum duration on the pump pulse duration τ_L/τ_R (the pulse durations normalized to the cavity trip time τ_R) at $R_S^{out} = 0.99, 0.70$, and 0.10

Figure 8 shows the calculated dependences of the parametrically generated pulse duration τ_{S2} , the pulse shortening relative value τ_L/τ_{S2} , and the quality of pulse shortening $\tau_{S2}/\Delta t$ on the pump level I_L^{in}/I_L^{th} at the pump pulse durations of $\tau_L = 2$ ns and $\tau_L = 6$ ns for the cavity output mirror reflectance at the first Stokes wavelength of $R_S^{out} = 99, 70$ and 10 %.

Figure 8 shows that for both $\tau_L = 2$ ns and $\tau_L = 6$ ns at the certain (optimum) pump level $(I_L^{in}/I_L^{th})_{opt}$ the shortened pulse with minimum duration $(\tau_{S2})_{min}$ shorter than 200 ps (Fig. 8a) can be obtained.

In the case of long pump pulse duration of $\tau_L = 6$ ns for a decrease in the generating pulse minimum duration $(\tau_{S2})_{min}$, an increase in the maximum relative value of the pulse shortening, and widening of the optimum range of the pump level $(I_L^{in}/I_L^{th})_{opt}$ is necessary to decrease the cavity output mirror reflectivity at the first Stokes wavelength down to $R_S^{out} = 10\%$.

In the case of short pump pulse duration of $\tau_L = 2$ ns, the decrease in R_S^{out} is not required, and the optimum range of the pump level $(I_L^{in}/I_L^{th})_{opt}$ is the widest.

Note that at the optimum pump level of $(I_L^{\text{in}}/I_L^{\text{th}})_{\text{opt}}$ not only the quantitative shortening (Fig. 8b: τ_L/τ_{S2} max) but also the quality of pulse shortening is the best (Fig. 8c: $\tau_{S2}/\Delta t$ close to unity).

Figure 9 presents the calculated dependences of the optimum pump level $(I_L^{\text{in}}/I_L^{\text{th}})_{\text{opt}}$, the minimum generated pulse duration $(\tau_{S2}/\tau_R)_{\text{min}}$, and the generation efficiency η_{S2}^{opt} of the pulse with minimum duration on the pump pulse duration τ_L/τ_R (the pulse durations normalized to the cavity transit time τ_R) at $R_S^{\text{out}} = 99, 70$ and 10% .

It is necessary to note that the calculation results presented in Fig. 9 are correct at any configurations of the internal cavity parametric Raman laser determined by the set of parameters $g, L, \tau_R, R_S^{\text{out}}$, and τ_L , because the durations (τ_L and τ_{S2}) are normalized to τ_R and the input pump intensity (I_L^{in}) is normalized to I_L^{th} (8).

Figure 9 shows the optimum pump level (Fig. 9a) corresponding to the minimum duration of the parametrically generated pulse increases with the pump pulse duration decrease. It results in decreasing the minimum duration of the parametrically generated pulse and increasing the generation efficiency of the pulse with the minimum duration (Fig. 9b).

The filled area of the graph (Fig. 9b) presents the optimum range of the normalized pump pulse duration values $(\tau_L/\tau_R)_{\text{opt}} < 30$ in which the minimum durations of the parametrically generated pulse $(\tau_{S2}/\tau_R)_{\text{min}}$ have the lowest values and the generation efficiency η_{S2}^{opt} of the pulse with the minimum duration has the highest values. In the optimum range of $(\tau_L/\tau_R)_{\text{opt}} < 30$ it is more efficient to use the high-reflective output mirror at the first Stokes wavelength ($R_S^{\text{out}} = 99\%$). Note that in the considered configuration of the parametric Raman laser (with $\tau_R = 66.7$ ps) the optimum boundary range of $(\tau_L/\tau_R)_{\text{opt}} = 30$ corresponds to the optimum pump pulse duration of $\tau_L = 2$ ns, and so the other considered cases of $\tau_L = 4$ ns and $\tau_L = 6$ ns are non-optimal.

Figure 9 shows that in the case of the non-optimal pump pulse durations from the range of $30 < \tau_L/\tau_R < 100$ a decrease in the output mirror reflectance R_S^{out} to 70% allows to generate shorter pulse with comparable (as for $R_S^{\text{out}} = 99\%$) generation efficiency decreasing with τ_L/τ_R . If $\tau_L/\tau_R > 100$, the shortest pulse is generated at lower $R_S^{\text{out}} = 10\%$, but the generation efficiency is very small.

5 Conclusions

In conclusion, a new effect of pulse shortening of the parametrically generated second Stokes Raman radiation down to 300 ps duration via the intracavity Raman conversion pumping depletion in the miniature passively Q-switched

Nd:SrMoO₄ parametric self-Raman laser with increasing the energy up to 1 μ J of the shortened pulse under pumping by the pulsed high-power laser diode bar is demonstrated. The second Stokes pulse is generated in the temporal region of the fundamental laser and first Stokes pulses overlap that is explained by the four-wave mixing mechanism of the second Stokes generation with the strongest nonlinear cavity dumping pulse shortening because of the fundamental radiation depletion terminating the four-wave-mixing generated second Stokes pulse. The theoretical study and mathematical modeling of this effect are carried out. The theoretical estimation of the convertible fundamental laser radiation depletion stage duration via intracavity Raman conversion (250 ps) is in agreement with the experimentally obtained duration of the parametrically generated pulse (280–300 ps). According to the mathematical modeling, the pulse shortening quality and quantity deterioration is disclosed and the solution ways are found by the laser parameters optimization. So, the ratio of the pump pulse duration to the cavity transit time should be lower than 30, and the input pulse intensity of intracavity pumping should be approximately by 5 times lower than the single-pass threshold pump intensity theoretically determined for any laser configuration.

Acknowledgments This research was supported by the Czech Science Foundation (Project No. 16-10019) and by the Russian Foundation for Basic Research (Grant No. 17-02-00452).

References

1. E. Granados, H.M. Pask, D.J. Spence, *Opt. Express* **17**, 569 (2009)
2. M. Murtagh, J. Lin, R.P. Mildren, G. McConnell, D.J. Spence, *Opt. Express* **23**, 15504 (2015)
3. M. Jelinek Jr., O. Kitzler, H. Jelinkova, J. Sulc, M. Nemeč, *Laser Phys. Lett.* **9**, 35 (2012)
4. M.E. Doroshenko, T.T. Basiev, S.V. Vassiliev, L.I. Ivleva, M.B. Kosmyna, J. Sulc, H. Jelinkova, *Opt. Mater.* **30**, 54 (2007)
5. T.T. Basiev, M.E. Doroshenko, L.I. Ivleva, I. Voronina, V. Konjushkin, V. Osiko, S.V. Vasilyev, *Opt. Lett.* **34**, 1102 (2009)
6. T.T. Basiev, S.V. Vassiliev, V.A. Konjushkin, V.V. Osiko, A.I. Zagumennyi, Y.D. Zavartsev, S.A. Kutovoi, I.A. Scherbakov, *Laser Phys. Lett.* **1**, 237 (2004)
7. C.C. Korel, J. Jakutis-Neto, D. Geskus, H. Pask, N. Wetter, *Opt. Lett.* **40**, 3524 (2015)
8. T.T. Basiev, S.N. Smetanin, A.V. Fedin, A.S. Shurygin, *Quantum Electron.* **40**, 704 (2010)
9. S.N. Smetanin, M. Jelnek Jr., V. Kubeek, H. Jelinkov, L.I. Ivleva, A.S. Shurygin, *Laser Phys. Lett.* **13**, 015801 (2016)
10. A.Z. Grasiuk, L.L. Losev, A.P. Lutsenko, S.N. Sazonov, *Sov. J. Quantum. Electron.* **20**, 1153 (1990)
11. R.P. Mildren, D.W. Coutts, D.J. Spence, *Opt. Express* **17**, 810 (2009)
12. A.Z. Grasiuk, S.V. Kubasov, L.L. Losev, *Opt. Commun.* **240**, 239 (2004)
13. S.N. Smetanin, T.T. Basiev, *Quantum Electron.* **42**, 224 (2012)

14. Y.R. Shen, *The Principles of Nonlinear Optics* (Wiley, New York, 1984)
15. N. Bloembergen, *Nonlinear Optics* (Benjamin Inc, New York, 1965)
16. R.L. Carman, F. Shimizu, C.S. Wang, N. Bloembergen, *Phys. Rev. A* **2**, 60 (1970)
17. T.T. Basiev, V.V. Osiko, A.M. Prokhorov, E.M. Dianov, *Top. Appl. Phys.* **89**, 351 (2003)
18. S.N. Smetanin, T.T. Basiev, *Opt. Spectrosc.* **114**, 813 (2013)
19. S.N. Smetanin, A.V. Fedin, A.S. Shurygin, *Quantum Electron.* **43**, 512 (2013)